Geomechanics and Engineering, *Vol. 25, No. 4 (2021) 317-330*
DOI: https://doi.org/10.12989/gae.2021.25.4.317

Predicting the unconfined compressive strength of granite using only two non-destructive test indexes

Danial J. Armaghani[1], Anna Mamou[2], Chrysanthos Maraveas[3], Panayiotis C. Roussis[4], Vassilis G. Siorikis[2], Athanasia D. Skentou[2] and Panagiotis G. Asteris[*2]

[1]*Department of Civil Engineering, Faculty of Engineering, University of Malaya, 50603, Kuala Lumpur, Malaysia*
[2]*Computational Mechanics Laboratory, School of Pedagogical and Technological Education, 15122 Marousi, Greece*
[3]*Department of Civil Engineering, University of Patras, Greece*
[4]*Department of Civil and Environmental Engineering, University of Cyprus, 1678 Nicosia, Cyprus*

(Received March 24, 2021, Revised April 19, 2021, Accepted May 12, 2021)

Abstract. This paper reports the results of advanced data analysis involving artificial neural networks for the prediction of the unconfined compressive strength of granite using only two non-destructive test indexes. A data-independent site-independent unbiased database comprising 182 datasets from non-destructive tests reported in the literature was compiled and used to train and develop artificial neural networks for the prediction of the unconfined compressive strength of granite. The results show that the optimum artificial network developed in this research predicts the unconfined compressive strength of weak to very strong granites (20.3-198.15 MPa) with less than ±20% deviation from the experimental data for 70% of the specimen and significantly outperforms a number of available models available in the literature. The results also raise interesting questions with regards to the suitability of the Pearson correlation coefficient in assessing the prediction accuracy of models.

Keywords: unconfined compressive strength; rocks; non-destructive testing; effective porosity, pulse velocity, artificial neural networks; machine learning

1. Introduction

The unconfined compressive strength of intact rock is a critical parameter in the Hoek and Brown (1997, 1980, 1983, 2002) constitutive model predicting the strength of a jointed rock mass. It has been shown that the unconfined compressive strength (UCS) depends on the intact rock's mineralogical composition, texture, fabric, specimen geometry, and rate of loading (Barton 1973, Hawkins 1998, Tsiambaos and Sabatakakis 2004). The unconfined compressive strength of intact rock can be determined in the laboratory following the detailed procedures outlined by the International Society for Rock Mechanics (ISRM 2007) and the American Society for Testing and Materials (ASTM 2016), which involve applying an increasing axial load on a ~2.5-3.0 height to diameter cylindrical intact rock specimen at a stress rate of ~0.5-1.0 MPa/s up to failure. Although the ISRM (2007) and ASTM (2016) standards provide detailed guidelines for eradicating possible size, shape, and strain-rate effects on the UCS of intact rock (Thuro *et al.* 2001), measuring the UCS in the laboratory is considered an elaborate destructive testing technique, requiring high-quality intact specimen free of cracks, fissures and veins, which are generally difficult to obtain from already significantly weak, fractured, and foliated rocks samples retrieved from the field.

A viable alternative, is to correlate the unconfined compressive strength of intact rock with other physical and mechanical properties, which are relatively easier to obtain, such as dry density (DD), effective porosity (n_e), compressional wave velocity (V_p), Schmidt hammer rebound number (R_n), and point load strength ($Is_{(50)}$) (Tuğrul and Zarif 1999, Kahraman 2001, Yasar and Erdogan 2004a, b, Aydin and Basu 2005, Çobanoğlu and Çelik 2008, Kılıç and Teymen 2008, Diamantis *et al.* 2009, Moradian and Behnia 2009, Dehghan *et al.* 2010, Mishra and Basu 2013, Ng *et al.* 2015, Tandon and Gupta 2015, Heidari *et al.* 2018). A variety of statistical analysis techniques, ranging from simple and multiple regression analysis to advanced data analysis involving artificial neural networks have been employed to predict the unconfined compressive strength of intact rock (Aggistalis *et al.* 1996, Armaghani *et al.* 2016a, b, Aladejare 2020, Ebdali *et al.* 2020, Tsiambaos and Sabatakis 2004, Yilmaz and Yuksek 2008, 2009, Khandelwal and Singh 2009, Singh *et al*. 2012, Momeni *et al.* 2015, Liang *et al.* 2016, Madhubabu *et al.* 2016, Li *et al.* 2020, Wang *et al.* 2020). Whilst a significant number of empirical relationships for the prediction of the unconfined compressive strength of intact rock have been proposed in the literature, the empirical models were generally fitted to a limited number of data (less than 182 datasets) which may have introduced a data-specific or site-specific bias, leading to over-fitting and hence unreliable parameter estimations (Ching *et al.* 2017, Bozorgzadeh *et al.* 2020). Another shortcoming of the empirical equations derived using simple regression analysis is their inability to simulate non-linear dependencies between input and output parameters

∗Corresponding author, Professor, Ph.D.
E-mail: asteris@aspete.gr

ISSN: 2005-307X (Print), 2092-6219 (Online)

with sufficient accuracy. To this end, soft computing techniques such as ANN may be successfully used to significantly improve the prediction accuracy of the unconfined strength of intact rock. During the last three decades, metaheuristic algorithms have been extensively used to simulate strongly non-linear relationships between numerous input parameters in several disciplines, such as in medicine research (Asteris *et al.* 2020, Rahimi *et al.* 2021, Gavriilaki *et al.* 2021) and in structural engineering applications (Zeng *et al.* 2021, Zhang *et al.* 2021, Zhao *et al.* 2021). Detailed and in-depth state-of-the-art reports on the use of neural networks in civil engineering applications are reported by Adeli (2001) and Kashani *et al.* (2020). A significant number of ANN models for the prediction of the unconfined compressive strength of rock have been proposed in the literature (Yılmaz and Yuksek 2008 and 2009, Dehghan *et al.* 2010, Yagiz *et al.* 2012, Ceryan *et al.* 2013, Minaeian and Ahangari 2013,Yesiloglu-Gultekin *et al.* 2013, Yurdakul and Akdas 2013, Momeni *et al.* 2015, Armaghani *et al.* 2016, a, b and c, Madhubabu *et al.* 2016, Ferentinou *et al.* 2017, Barham *et al.* 2020, Ceryan and Samui 2020, Ebdali *et al.* 2020, Teymen and Menguc 2020, Moussas and Diamantis 2021). The aim of this paper is to consolidate the results from numerous non-destructive tests reported in the literature into a data-independent site-independent unbiased database comprising 182 datasets, which was used to train and develop artificial neural networks for the prediction of the unconfined compressive strength of rock using the effective porosity, η_e, and compressional wave velocity, Vp, as input parameters.

2. Research significance

Predicting the unconfined compressive strength of rock from non-destructive tests is a viable alternative to direct laboratory measurements, which require high quality specimen free of cracks and fissures which are generally difficult to obtain from fractured rock samples retrieved from the field. Whilst a significant number of empirical relationships for the prediction of the unconfined compressive strength of rock have been proposed, the models were generally fitted to a limited number of data (less than 182 datasets), which may have introduced a data-specific or site-specific bias leading to over-fitting and hence unreliable parameter estimations. The aim of this paper is to consolidate the results from numerous non-destructive tests reported in the literature, into a data-independent site-independent unbiased database comprising 182 datasets, which was used to train and develop artificial neural networks for the prediction of the unconfined compressive strength of rock.

3. Literature review on the available proposals for the unconfined compressive strength of rocks

3.1 Experimental works

The constitutive models predicting the strength of a jointed rock mass are highly nonlinear and anisotropic, and generally require the determination of the unconfined compressive strength of intact rock and of dimensionless strength parameters, which depend on the shape of the intact rock pieces and the condition of the separating block surfaces (Hoek and Brown 1980, 1983 and 2002, Marinos and Hoek 2000). The unconfined strength of intact rock may be obtained by either direct laboratory measurements or by correlating the unconfined strength of rock with the results from physical and mechanical index tests. In this research, the unconfined compressive strength of rock is predicted using only two input parameters, the effective porosity, η_e, and the compressional wave velocity, V_p. Both indexes are obtained from non-destructive tests, alleviating the need for high-quality intact specimen free of cracks, fissures, and veins.

Effective porosity η_e

Porosity is a fundamental physical property, which quantifies the presence of voids in the form of intergranular space, microfractures at grain boundaries, joints and faults (Franklin and Dusseault 1991). The effective porosity, η_e, defined as the fraction of the volume of voids that are fully interconnected, is calculated as

$$\eta_e = \left(\frac{M_{sat}-M_{dry}}{M_{sat}-M_{sus}}\right) x100\% \quad (1)$$

where M_{sat} is the saturated mass, M_{su} the suspended mass, and M_{dry} the dry mass. The effective porosity η_e, may be measured by initially applying a vacuum and then gradually permeating the specimen with deaired water until it is completely submerged under water. The porosity of rocks if influenced by the grain size, packing, grain distribution, particle shape and degree of weathering, which may change the pore size distribution, pore geometry, and even result in new pore formation (Tugrul 2004, Chaki *et al.* 2008).

Compressional wave velocity V_p

The pulse velocity test is a non-destructive test which involves the propagation of compressional and/or shear wave velocities below the yield stress of rocks. The compressional wave velocity V_p is measured by propagating low-amplitude compressional waves between a transmitter and a receiver and measuring the required travel time. The compressional wave velocity depends on the mineralogical composition, texture, fabric, degree of weathering, water content, and density of rock (Yasar and Erdogan 2004, Kilic and Teymen 2008, Dheghan *et al.* 2010, Mishra and Basu 2013, Momeni *et al.* 2015, Ng *et al.* 2015, Tandon and Gupta 2015, Heidari *et al.* 2018).

3.2 Available proposals

Interestingly, although numerous relationships have been proposed for the prediction of the unconfined compressive strength of rock using either the effective porosity or the compressional wave velocity as input parameters, only a limited number of relationships have been proposed using both input parameters (Table 1). The proposed correlations of effective porosity and compressive wave velocity with the unconfined compressive strength of rock have been proposed using simple regression analysis (for example, Sousa *et al.* 2005, Mishra and Basu 2013) and hierarchical Bayesian modelling (Ng *et al.* 2015). The proposed relationships span the very-low- to low-porosity

Table 1 Available proposals correlating effective porosity and compressional wave velocity with the unconfined compressive strength of granite

Empirical relationship	Equation	Method	Reference	Range of parameters		
				ne	vp	UCS
$UCS=124.28\ n_e^{-0.56}$	(2)	RA	Sousa *et al.* (2005)	0.6-3.7	-	60-200MPa
$UCS=0.004Vp^{1.247}$	(3)	RA	Sousa *et al.* (2005)	-	2500-5900m/s	60-200MPa
UCS=0.0407Vp-36.31	(4)	RA	Vasconcelos *et al.* (2008)	-	1956-4804m/s	35.2-159.8MPa
UCS=0.087Vp-355.8	(5)	RA	Mishra and Basu (2013)	-	5500-6400m/s	17.55-198.15MPa
$UCS=228.2e^{(-1.98ne)}$	(6)	RA	Mishra and Basu (2013)	0.05-0.4	-	17.55-198.15MPa
$UCS= -17.88\ln(n_e)+60.22$	(7)	BHM	Ng *et al.* (2015)	0.52-7.23	-	20.3-112.9MPa
$UCS=8.17e^{0.0004Vp}+3.93$	(8)	BHM	Ng *et al.* (2015)	-	1160-5935m/s	20.3-112.9MPa
$UCS=6.32e^{0.0004Vp}-9.6\ln(n_e)+20.5$	(9)	BHM	Ng *et al.* (2015)	0.52-7.23	1160-5935m/s	20.3-112.9MPa
UCS=0.0218Vp-15.421	(10)	RA	Armaghani *et al.* (2016a)	-	2823-7943m/s	39-211.9MPa
$UCS=26.449e^{0.0003Vp}$	(11)	RA	Armaghani *et al.* (2016a)	-	2823-7943m/s	39-211.9MPa
$UCS=0.005Vp^{1.141}$	(12)	RA	Armaghani *et al.* (2016a)	-	2823-7943m/s	39-211.9MPa
UCS=103.98ln(Vp)-788.890	(13)	RA	Armaghani *et al.* (2016a)	-	2823-7943m/s	39-211.9MPa

RA: Regression Analysis; BHM: Bayesian Hierarchical Modelling

range (n_e = 0.05-7.23). The unconfined compressive strength of rock is generally proposed to reduce logarithmically with increasing effective porosity, whereas linear exponential and power relationships have been generally proposed for the correlation of the compressive wave velocity and unconfined compressive strength. The unconfined compressive strength of granite spans the weak to very-strong range (ISRM 2007).

4. Materials and methods

4.1 Artificial neural networks

This section presents the underlying principles and constitutive modeling rules underpinning artificial neural networks. ANNs are advanced numerical models mimicking the structure and interaction of biological neural networks. At present, most neural network models presented in the literature are structured using coarse elements of the biological neural networks, and in this context it is expected that artificial neural network models will in the future be refined as the functions underpinning biological neurons advance.

Artificial neural networks are robust soft computing models which can simulate complicated non-linear associations between a series of input and output parameters (Hornik *et al.* 1989, Samui 2008, Das *et al*. 2011, Samui and Kothari 2011, Asteris and Plevris 2013 and 2016, Nikou *et al.* 2016, 2017 and 2018, Asteris and Kolovos, 2017, Asteris *et al.* 2017, Cavaleri *et al.* 2017, Psyllaki *et al.* 2018, Apostolopoulou *et al*. 2018, 2019 and 2020, Kechagias *et al.* 2018, Armaghani *et al.* 2019, Asteris and Mokos 2019, Cavaleri *et al.* 2019, Chen *et al.* 2019, Xu *et al.* 2019). In this research, back-propagation neural networks (BPNNs) were trained and developed for the prediction of the unconfined compressive strength of granite. A BPNN is a feed-forward, multilayer network (Hornik *et al.* 1989), in which information flows only from the input towards the output nodes with no feedback loops, while the neurons of the same layer are not interconnected with each other but are connected with all the neurons of the previous and subsequent layer. The architecture of a BPNN can be expressed as

$$N - H_1 - H_2 - \cdots - H_{NHL} - M \quad (2)$$

where N is the number of input neurons (input parameters), H_i is the number of neurons in the ith hidden layer for i =1, …, NHL, NHL is the number of hidden layers, and M is the number of output neurons (output parameters).

Despite the fact that the majority of researchers employing ANN techniques use multilayer NN models, ANN models comprising only one hidden layer can predict any forecast problem in an equally reliable and robust manner.

A typical structure of a single node (with the corresponding R-element input vector) of a hidden layer is presented in Fig. 1.

For each neuron i, the individual element inputs

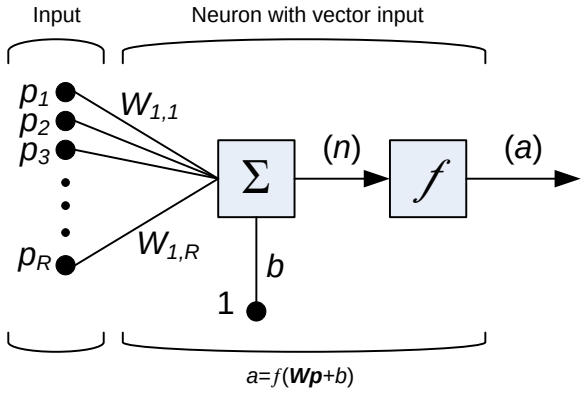

Fig. 1 Architecture of a neuron with a single input vector

$p_1, \dots, p_R$ are multiplied with the corresponding weights $w_{i,1}, \dots, w_{i,R}$ and the weighted values are fed to the junction of the summation function, where the dot product $(W \cdot p)$ of the weight vector $W = [w_{i,1}, \dots, w_{i,R}]$ and the input vector $p = [p_1, \dots, p_R]^T$ is generated. The threshold b (bias) is added to the dot-product forming the net input n, which is the argument of the transfer function f:

$$n = W \cdot p = w_{i,1}p_1 + w_{i,2}p_2 + \dots + w_{i,R}p_R + b \quad (3)$$

The choice of the transfer (or activation) function f may significantly influence the complexity and performance of ANN. Although sigmoidal transfer functions are the most commonly used, different types of functions are available. For example, Bartlett (1998) and Karlik and Olgac (2011) proposed a significant number of alternative transfer functions. In this research, the Logistic Sigmoid and the Hyperbolic Tangent transfer functions were considered to be more suitable for the specific research topic. During the training phase, the training data are fed into the network which gradually builds correlations between the input and the output values. This correlation is achieved by adjusting the weights in order to minimize the following error function

$$E = \sum (x_i - y_i)^2 \quad (4)$$

where x_i and y_i are the measured values and the prediction of the network, respectively, within an optimization framework.

In this research, an in-depth investigation was carried out based on (i) a plethora of different architectures, and (ii) ten different activation functions which will be presented and discussed in a following section. This resulted in 100 (10×10) different combinations being applied during the training and development stage of the BPNNs.

4.2 Experimental database

It should be noted that the term "sufficient amount of data" does not necessarily imply a high amount of data, but rather datasets that cover a wide range of combinations of input parameter values, thus assisting in the model capability to simulate the problem. The demand for a reliable database is particularly crucial in the case of experimental databases, which are databases which are compiled using experimental results. In this case, significant deviations between experimental values are frequently noticed, not only between experiments conducted by different research teams and laboratories, but even between datasets derived from experiments conducted on specimens of the same synthesis, produced by the same technicians, cured under the same conditions and tested implementing the same standards and the same testing instruments.

In light of the above discussion, an experimental database comprising 182 datasets was compiled from the following research papers reported in the literature (Tuğrul and Zarif 1999, Mishra and Basu 2013, Ng *et al.* 2015). Table 2 presents in detail the number of samples and the range of unconfined compressive strength for each one

Table 2 Data from experiments published in literature

Reference	Number of Samples	Unconfined Compressive Strength UCS in MPa
Tuğrul and Zarif (1999)	19	109.17-193.33
Mishra and Basu (2013)	18	91.48-198.15
Ng *et al.* (2015)	145	20.30-112.90
Total	182	20.30-198.15

Table 3 Correlation matrix of the input and output variables

Variable		Input		Output
Input	ne %	1,00		
	Vp	-0.62	1.00	
Output	UCS	-0.58	0.81	1.00

Table 4 The input and output parameters used in the development of soft computing model for the prediction of unconfined compressive strength of rock

Variable	Symbol	Units	Category	Statistics			
				Min	Average	Max	STD
Effective Porosity	n_e %	-	Input	0.06	1.67	7.23	1.47
Compressional Wave Velocity	Vp	m/s	Input	1160.00	4611.79	6690.00	985.18
Unconfined Compressive Strength UCS	UCS	MPa	Output	20.30	73.56	198.15	43.87

experimental work used for the compilation of the database which will be used for the development and training of soft computing model such as artificial neural networks. Each dataset comprises two input parameters (effective porosity, n_e and compressional wave velocity, Vp) and the unconfined compressive strength (UCS) as the output parameter. Dry specimens were used to measure the compressional wave velocity and unconfined compressive strength, eradicating any water content effects (Tuğrul and Zarif 1999, Mishra and Basu 2013, Ng *et al.* 2015). Table 3 presents the correlation matrix of the input and output parameters while Table 4 shows the minimum average and maximum values, as well as the standard deviation of the input and output parameters respectively. The histograms for each of the input and output parameters presented in Fig. 2 shows that the consolidated database spans the very weak to strong rock range (Goudie 2006).

4.3 Sensitivity analysis of the unconfined compressive strength of the experimental database

A sensitivity analysis identifies which input parameters have an insignificant effect on the predicted output parameter, so as to remove them from the analysis, thus reducing the input space and complexity of the model together with the required training time. In this research, a sensitivity analysis was performed using the cosine amplitude method (CAM) which has been used by numerous researchers (Armaghani *et al.* 2015, Momeni *et al.* 2015, Khandelwal *et al.* 2016, Zeng *et al.* 2021). In

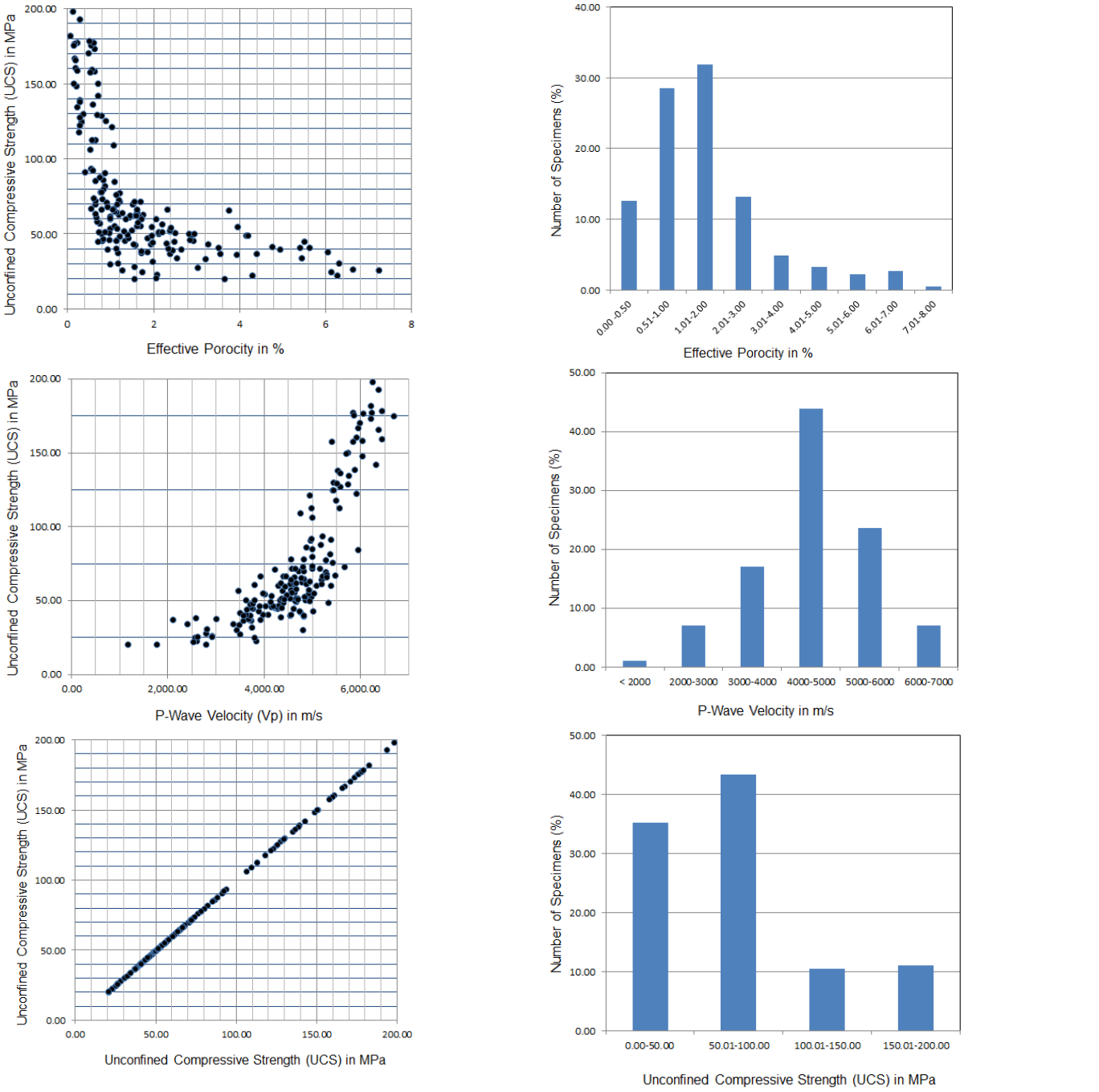

Fig. 2 Histograms of the input and output parameters

CAM, data pairs may be used to construct a data array, X, as follows:

$$X = \{x_1, x_2, x_3, \dots, x_i, \dots, x_n\} \quad (5)$$

Variable x_i in array X is a length vector of m expressed as:

$$x_i = \{x_{i1}, x_{i2}, x_{i3}, \dots, x_{im}\} \quad (6)$$

The relationship between R_{ij} (strength of the relation) and datasets of x_i and x_j may be expressed as:

$$R_{ij} = \frac{\sum_{k=1}^{m} x_{ik}x_{jk}}{\sqrt{\sum_{k=1}^{m} x^2_{ik} \sum_{k=1}^{m} x^2_{ik}}} \quad (7)$$

The R_{ij} values of the compressive strength and the input parameters are shown in Fig. 3. The results show that the compressional wave velocity registered a strength index of 0.92 and had a higher influence on the unconfined compressive strength of granite as compared to the effective porosity which registered a relative strength index of 0.45.

4.4 Performance indexes

Three different statistical performance indexes were used to assess the performance of the ANN models including the root mean square error (RMSE), the mean absolute percentage error (MAPE), and the Correlation

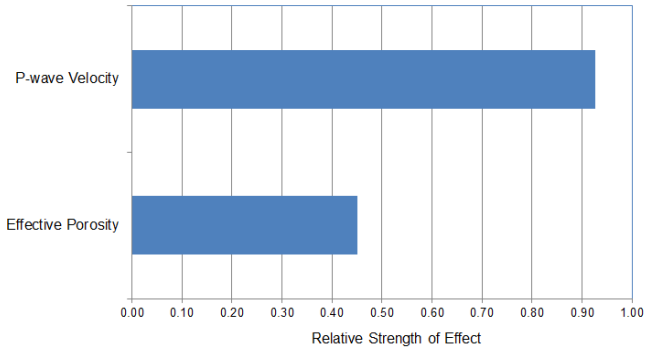

Fig. 3 Sensitivity analysis of the unconfined compressive strength on input parameters based on the experimental database

Coefficient (R^2). Lower RMSE and MAPE values indicate more accurate predictions (a null value indicates a perfect fit), while higher R values indicate a better fit between the measured and predicted values (a zero value indicates no fit, and a unit value indicates a perfect fit). The aforementioned statistical parameters have been calculated using the following expressions (Alavi and Gandomi 2012):

$$RMSE = \sqrt{\frac{1}{n}\sum_{i=1}^{n}(x_i - y_i)^2} \quad (8)$$

$$MAPE = \frac{1}{n}\sum_{i=1}^{n}\left|\frac{x_i - y_i}{x_i}\right| \quad (9)$$

$$R^2 = 1 - \left(\frac{\sum_{i=1}^{n}(x_i - y_i)^2}{\sum_{i=1}^{n}(x_i - \bar{x})^2}\right) \quad (10)$$

where, n denotes the total number of datasets, and x_i and y_i represent the predicted and target values, respectively.

The reliability and accuracy of the developed neural networks were evaluated using R^2 and RMSE. RMSE presents information on the short-term efficiency, which is a benchmark of the difference of predicated values in relation to the experimental values. R^2 measures the variance that is interpreted by the model, which is the reduction of variance when using the model. It should be noted that, amongst the statistical indexes available, the majority of researchers use the R^2 in order to evaluate the effectiveness of the developed computation model. R^2 is a measure of the linear correlation between two variables X and Y. For forecasting models, such as neural network models, X and Y represent the measured and predicted values, respectively. According to the Cauchy–Schwarz inequality (Wu and Wu 2009), the coefficient R has a value between +1 and −1. The further away R is from zero, the stronger the linear relationship is between the two variables. The sign of R corresponds to the direction of the relationship. If R is positive, then as one variable increases, the other variable tends to increase. If R is negative, then as one variable increases, the other variable tends to decrease. A perfect linear relationship (R = –1 or R = +1) means that one of the variables can be perfectly expressed as a linear function of the other. As aforementioned, the reliability of a model's forecasting ability increases as the R^2 value approaches the unit value. Despite the fact that this index is widely used by the majority of researchers, it is in fact the most unreliable amongst the available statistical indices.

When two forecasting models present different R values, as well as different slope values, comparison between the models is impossible. Even more so, when evaluating neural networks developed through different architectures. Therefore, the a20-index, has been recently proposed (Apostolopoulou *et al.* 2019 and 2020, Asteris and Mokos 2019, Armaghani *et al.* 2020, Armaghani and Asteris 2020, Asteris *et al.* 2020) for assessing the developed soft computing techniques reliability:

$$a20 - index = \frac{m20}{M} \quad (11)$$

where, M is the number of dataset sample and m20 is the number of samples with a value of (experimental value)/(predicted value) ratio, between 0.80 and 1.20. Note that for a perfect predictive model, the values of a20-index values are expected to be the unit value. The proposed a20-index has the advantage of a physical engineering meaning, as it shows the amount of samples that satisfy the predicted values with a deviation of ±20%, compared to experimental values.

4.5 Methodology

Numerous ANN architectures correlating the effective porosity and the compressional wave velocity with the unconfined compressive strength of intact rock were investigated. The various ANN were ranked using the performance indexes presented in the previous section and the optimum ANN should minimize any overfitting issues. The architecture of the trained and developed ANN used in this research will not be limited to the following three commonly-used transfer functions Hyperbolic Tangent Sigmoid transfer function (HTS), Log-sigmoid transfer function (LS), and Linear transfer function (Li). In this study, a total of 10 functions is used in each hidden layer, resulting in NNs comprising one hidden layer with 100 (10×10) different structures for each developed architecture of ANNs. Four different normalization techniques were applied to both input and output parameters.

5. Results and discussion

5.1 Development and training of ANN models

A number of normalization techniques and transfer functions for the training and development of BPNN were investigated (Table 5). Typical architectures for each normalization technique and the predictive performance of each model when only the testing datasets are used is presented in Table 6. The results show the significance of the employed transfer functions on the prediction accuracy of the models. For example, BPNN2-6-1, comprises only 6 neurons and has a better prediction accuracy in terms of both R and RMSE than BPNN 2-20-1 which comprises 20 neurons, but utilizes different transfer functions.

Table 5 Training parameters of ANN models

Parameter	Value
Training Algorithm	Levenberg-Marquardt Algorithm
Normalization	Minmax in the range 0.10 – 0.90 Minmax in the range -1.00 –10.90 Zscore
Number of Hidden Layers	1
Number of Neurons per Hidden Layer	1 to 20 by step 1
Control random number generation	10 different random generation
Training Goal	0
Epochs	250
Cost Function	Mean Square Error (MSE) Sum Square Error (SSE)
Transfer Functions	Hyperbolic Tangent Sigmoid transfer function (HTS) Log-sigmoid transfer function (LS) Linear transfer function (Li) Positive linear transfer function (PLi) Symmetric saturating linear transfer function (SSL) Soft max transfer function (SM) Competitive transfer function (Co) Triangular basis transfer function (TB) Radial basis transfer function (RB) Normalized radial basis transfer function (NRB)

Table 6 Best Architectures for each normalization technique based on the RMSE using only the testing datasets

Case	Normalization Technique	Cost Function	Transfer Function		Architecture	Performance Indexes	
			Hidden Layer	Output Layer		R	RMSE
I	no	'MSE'	HTS	PLi	BPNN 2-20-1	0.9660	11.8544
II	minmax [0.10, 0.90]	'SSE'	SSL	RB	BPNN 2-14-1	0.9657	11.8711
III	minmax [-1.00, 1.00]	'SSE'	NRB	HTS	BPNN 2-6-1	0.9695	11.3454
IV	**zscore**	**'SSE'**	**TB**	**Li**	**BPNN 2-17-1**	**0.9722**	**10.6871**

HTS : Hyperbolic Tangent Sigmoid transfer function (HTS); PLi : Positive linear transfer function; Li :Linear transfer function; SSL : Symmetric saturating linear transfer function; RB : Radial basis transfer function; NRB : Normalized radial basis transfer function; TB : Triangular basis transfer function (TB)

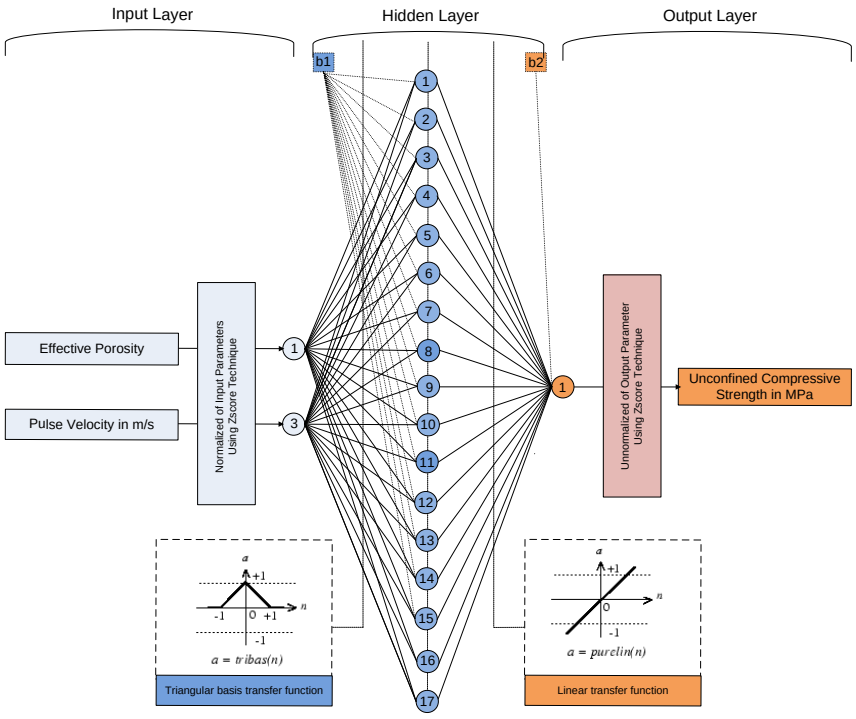

Fig. 4 Architecture of the optimum BPNN 2-17-1 model

5.2 Optimum ANN model

The BPNN2-17-1 has the highest prediction accuracy of all the PBNNs developed in this research. The architecture of the BPNN2-17-1 model is presented in detail in Fig. 4. BPNN2-17-1 correlates the unconfined compressive strength of granite with the effective porosity and compressional wave velocity using 17 hidden neurons. A triangular basis transfer function (TB) was used as a hidden layer and a Linear transfer function as an output layer. Table

Table 7 Summary of prediction capability of the optimum 2-17-1 BPNN

Model	Data sets	Performance Indices				
		a20-index	R	RMSE	MAPE	VAF
BPNN 2-17-1	Training	0.7377	0.9600	12.7009	0.1424	91.8016
	Testing	0.7000	0.9722	10.6871	0.1297	94.4739
	All	0.6923	0.9551	13.1690	0.1533	90.9455

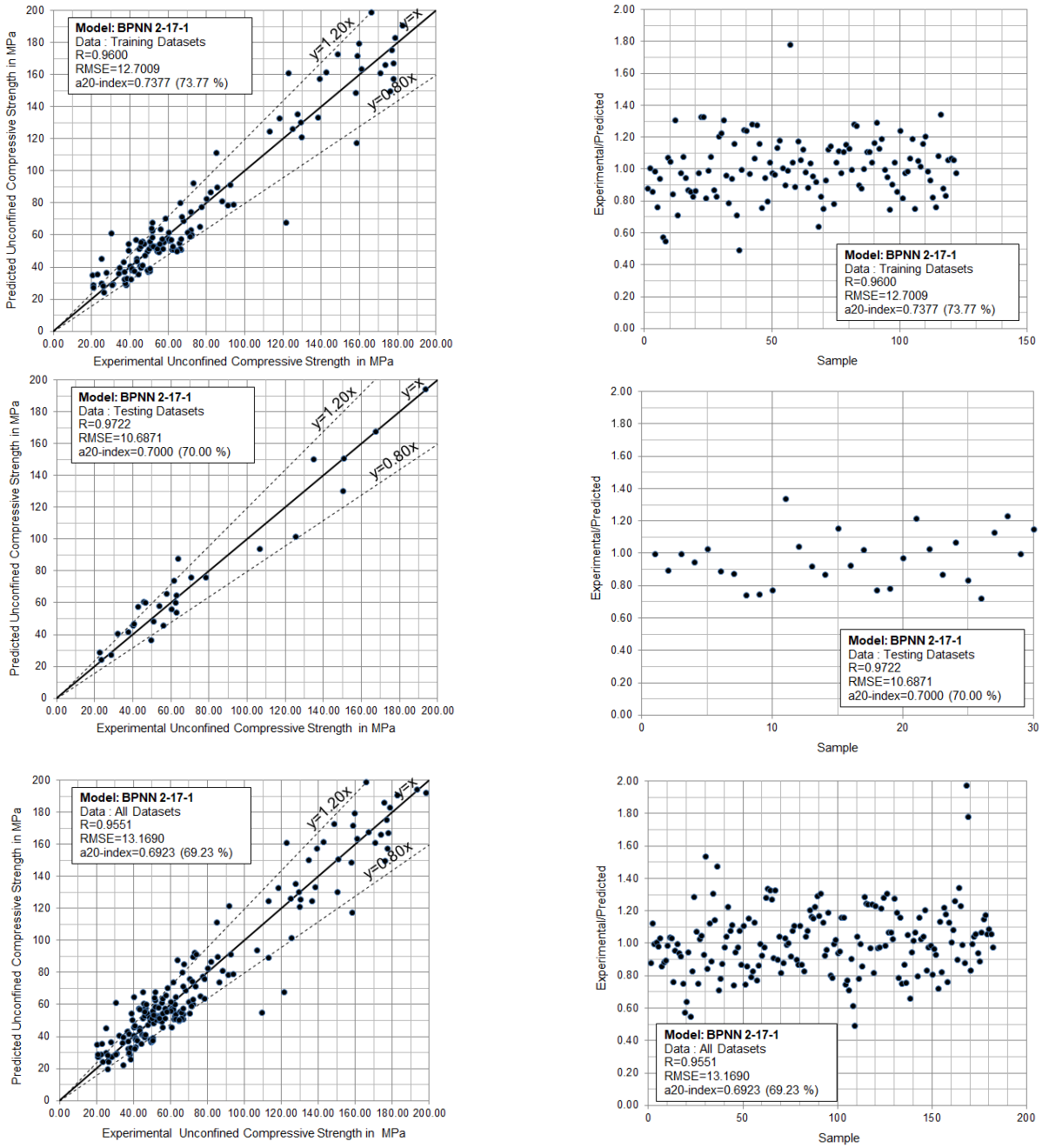

Fig. 5 Experimental vs predicted values of the unconfined compressive strength based on the optimum BPNN 2-17-1

Table 8 Ranking of the prediction accuracy of the optimum BPNN-2-17-1 model and typical analytical solutions proposed in the literature based on a20-index and testing datasets

Ranking	Model	Equation	Method	Performance Indexes		
				a20-index	R	RMSE
1	BPNN 2-17-1	24	BPNN	0.7000	0.9722	10.6871
2	Ng *et al.* (2015)	8	BHM	0.5667	0.9293	31.5866
3	Ng *et al.* (2015)	9	BHM	0.5667	0.9298	27.7717
4	Ng *et al.* (2015)	7	BHM	0.4667	0.7958	35.9029
5	Mishra and Basu (2013)	5	RA	0.3333	0.8423	55.0519
6	Mishra and Basu (2013)	6	RA	0.3000	0.8379	38.7182
7	Armaghani *et al.* (2016a)	11	RA	0.2333	0.9135	42.6706
8	Armaghani *et al.* (2016a)	13	RA	0.1667	0.7663	33.7077
9	Armaghani *et al.* (2016a)	12	RA	0.1667	0.8516	31.9605
10	Sousa *et al.* (2005)	2	RA	0.1000	0.8175	84.7516
11	Armaghani *et al.* (2016a)	10	RA	0.1000	0.8423	32.6020
12	Sousa *et al.* (2006)	3	RA	0.0667	0.8583	79.5723
13	Vasconcelos *et al.* (2008)	4	RA	0.0667	0.8423	82.0170

BPNN: Back Propagation Neural Network; BHM: Bayesian Hierarchical Modelling; RA: Regression Analysis

7 shows that during the training stage BPNN 2-17-1 predicts the unconfined compressive strength of granite with less than ±20% deviation from the experimental datafor 73.77% of the specimen, and when all the data are included in the simulation the prediction accuracy reduces slightly to less than ±20% deviation from the experimental data for 69.23% of the specimen. Moreover, the Experimental vs Predicted values of the Unconfined Compressive Strength based on the Optimum BPNN 2-17-1 can be seen in Fig. 5.

5.3 Proposed explicit equation based on the optimum ANN model

In most previous studies investigating the training and development of artificial neural networks, the final values of ANN weights and biases were generally not reported. Therefore, it is challenging for other researchers and practicing engineers to reproduce the results, which renders the applicability of the reported models limited. To address this issue, this research presents the (quantitative) values of weights, so that the proposed ANN scheme can be readily implemented in a spreadsheet and be accessible to everyone interested in the procedure of simulation.

This section presents the closed form of the explicit equations for the prediction of the unconfined compressive strength of granite. It is not convenient for engineers/researchers to use machine learning models in practice, because such a "black-box" model comprises weights and biases, together with activation functions. Thus, explicit equations based on the developed back propagating neural network should be derived for a direct and efficient application. The proposed equation for the prediction of the unconfined compressive strength (UCS) of granite using the effective porosity, n_e, and the compressional wave velocity, V_p, as input parameters may be expressed as the following matrix:

$$\mathrm{UCS} = purelin([L_W] \times [tribas([I_W] \times [IP] + [b_i])] + [b_0])\sigma + \mu \quad (12)$$

where purelin is the Linear transfer function and tribas is the Triangular basis transfer function. $[\mathrm{I_W}]$ is a 17×2 matrix containing weights of the hidden layer; $[\mathrm{L_W}]$ is a 1×17 vector containing weights of the output layer; $[IP]$ is a 2×1 vector of the 2 Input Parameters, $[\mathrm{b_i}]$ is a 17×1 vector containing the bias of the hidden layer; and $[\mathrm{b_0}]$ is a 1×1 vector containing the bias of the output layer. $\sigma = 43.87$ is the standard deviation of the unconfined compressive strength, and $\mu = 73.56$ is the mean value of the unconfined compressive strength.

The $[\mathrm{I_W}]$ may be expressed as:

$$[I_W] = \begin{bmatrix} -1.1616 & -0.9250 \\ 0.1198 & -1.5096 \\ -0.6893 & -0.1715 \\ 2.0211 & -0.1195 \\ -0.3689 & -0.1197 \\ -1.5842 & -1.0645 \\ -2.0658 & 0.1307 \\ 0.1764 & -2.3631 \\ 0.3787 & -1.5379 \\ 4.1071 & -1.0021 \\ -3.3187 & 5.8188 \\ 0.4035 & -0.7106 \\ -0.7891 & -0.0460 \\ 0.2340 & 1.2602 \\ 0.2184 & 1.1279 \\ -0.2534 & 1.0124 \\ 0.6060 & -0.3457 \end{bmatrix} \quad (13)$$

while the $[\mathrm{L_W}]$, $[\mathrm{b_i}]$ and $[\mathrm{b_0}]$ may be expressed as:

$$[L_W]^T = \begin{bmatrix} 0.5447 \\ 0.8552 \\ 0.4399 \\ 0.2139 \\ 0.5603 \\ 0.3870 \\ 0.4493 \\ 0.1288 \\ 0.0864 \\ 0.0057 \\ -0.7554 \\ 0.9357 \\ -1.2383 \\ -0.8806 \\ 0.8791 \\ -0.3782 \\ 3.8834 \end{bmatrix} \quad [b_i] = \begin{bmatrix} 4.7483 \\ 3.9381 \\ 1.6015 \\ -4.7763 \\ -0.6939 \\ 0.3317 \\ 3.2438 \\ -2.7696 \\ -1.0645 \\ -1.8088 \\ -5.8411 \\ -0.0059 \\ -1.4957 \\ 0.1162 \\ 0.0485 \\ -0.2969 \\ 1.2307 \end{bmatrix} \quad (14)$$

$$[b_0] = [-1.3712] \quad (15)$$

The $[IP]$ vector of the 2 Input Parameters (porosity n_e, and the pulse velocity V_p) may be expressed as

$$[IP] = \begin{bmatrix} \frac{(n_e - 1.67)}{1.47} \\ \frac{(V_p - 4611.79)}{985.18} \end{bmatrix} \quad (16)$$

5.4 Comparison of the proposed model with other available proposals

Table 8 compares the prediction accuracy of the BPNN 2-17-1 developed in this research with a number of available equations reported in the literature. The various models are ranked based on their a20-index for the case of testing datasets, but the performance of the Pearson correlation coefficient R and the RMSE is also presented. The results show that the BPNN 2-17-1 outperforms all the available models regardless of which performance index is used. The results also raise interesting questions with regards to the suitability of the Pearson correlation coefficient in assessing the prediction accuracy of models. For example although the Pearson correlation coefficient of the BPNN-2-17-1 and the Vasconcelos *et al.* (2008) model differ by only 15%, the BPNN 2-17-1 model predicts the UCS of granite with less than ±20% deviation from the experimental data for 70% of the specimen, whereas the Vasconcelos *et al.* (2008) model predicts the UCS of granite with less than ±20% deviation from the experimental data for only 6.67% of the specimen.

6. Conclusions

The aim of this research was to outperform the predictive accuracy of the models currently available in the literature, which use the effective porosity and/or the compressional wave velocity as the only input parameters for the prediction of the unconfined compressive strength of granite. To this end, a series of BPNN using various normalization techniques and transfer functions were trained and developed. The following main conclusion may be drawn:

• The BPNN2-17-1 developed in this research provides a more accurate prediction of the UCS of granite as compared to the predicted UCS proposed by the Sousa et al. (2005), Vasconcelos *et al.* (2008), Mishra and Basu (2013), Ng *et al.* (2015), Armaghani *et al.* (2016a) models, regardless of which performance index is used (a-20, R, RMSE).

• The BPNN2-17-1 predicts the unconfined compressive strength of weak to very strong granites ranging between 20.3-198.15 MPa with less than ±20% deviation from the experimental data for 70% of granite specimens.

• The results raise interesting questions with regards to the suitability of the Pearson correlation coefficient, R, in assessing the prediction accuracy of the models. For example, although the Pearson correlation coefficient of the BPNN-2-17-1 and the Vasconcelos *et al.* (2008) model differ by only 15%, the BPNN 2-17-1 model predicts the UCS of granite with less than ±20% deviation from the experimental data for 70% of the specimen, whereas the Vasconcelos *et al.* (2008) model predicts the UCS of granite with less than ±20% deviation from the experimental data for only 6.67% of the specimen.

• To illuminate the "black box" of the developed BPNN2-17-1, the final values of the ANN weights and biases are presented as a closed form equation (24), which can be used as a basis to refine the accuracy of the BPNN2-17-1 over an extended database.

References

Adeli, H. (2001), "Neural networks in civil engineering: 1989-2000", *Comput-Aid. Civ. Infrastruct. Eng.*, **16**, 126-142. https://doi.org/10.1111/0885-9507.00219.

Aggistalis, G., Alivizatos, A., Stamoulis, D. and Stournaras, G. (1996), "Correlating uniaxial compressive strength with Schmidt hardness, point load index, Young's modulus, and mineralogy of gabbros and basalts (Northern Greece)", *B. Int. Assoc. Eng. Geol.*, **54**(1), 3-11. https://doi.org/10.1007/BF02600693.

Aladejare, A.E. (2020), "Evaluation of empirical estimation of uniaxial compressive strength of rock using measurements from

Alavi, A.H. and Gandomi, A.H. (2012), "Energy-based numerical models for assessment of soil liquefaction", *Geosci. Front.*, **3**(4), 541-555. https://doi.org/10.1016/j.gsf.2011.12.008.

Apostolopoulou, M., Armaghani, D.J., Bakolas, A., Douvika, M.G., Moropoulou, A. and Asteris, P.G. (2019), "Compressive strength of natural hydraulic lime mortars using soft computing techniques", *Proc. Struct. Integrit.*, **17**, 914-923. https://doi.org/10.1016/j.prostr.2019.08.122.

Apostolopoulou, M., Asteris, P.G., Armaghani, D.J., Douvika, MG., Lourenço, P.B., Cavaleri, L., Bakolas, A. and Moropoulou, A. (2020), "Mapping and holistic design of natural hydraulic lime mortars", *Cement Concrete Res.*, **136**, 106167. https://doi.org/10.1016/j.cemconres.2020.106167.

Apostolopoulou, M., Douvika, M.G., Kanellopoulos, I.N., Moropoulou, A. and Asteris, P.G. (2018), "Prediction of compressive strength of mortars using artificial neural networks", *Proceedings of the 1st International Conference TMM_CH, Transdisciplinary Multispectral Modelling and Cooperation for the Preservation of Cultural Heritage*, Athens, Greece, October.

Armaghani, D.J. and Asteris, P.G. (2020), "A comparative study of ANN and ANFIS models for the prediction of cement-based mortar materials compressive strength", *Neural Comput. Appl.*, 1-32. https://doi.org/10.1007/s00521-020-05244-4.

Armaghani, D.J., Amin, M.F.M., Yagiz, S., Faradonbeh, R.S. and Abdullah, R.A. (2016c), "Prediction of the uniaxial compressive strength of sandstone using various modeling techniques", *Int. J. Rock Mech. Min. Sci.*, **85**, 174-186. https://doi.org/10.1016/j.ijrmms.2016.03.018.

Armaghani, D.J., Hajihassani, M., Sohaei, H., Mohamad, E.T., Marto, A., Motaghedi, H. and Moghaddam, M.R. (2015), "Neuro-fuzzy technique to predict air-overpressure induced by blasting", *Arab. J. Geosci.*, **8**(12), 10937-10950. https://doi.org/10.1007/s12517-015-1984-3.

Armaghani, D.J., Hatzigeorgiou, G.D., Karamani, Ch., Skentou, A., Zoumpoulaki, I. and Asteris, P.G. (2019), "Soft computing-based techniques for concrete beams shear strength", *Proc. Struct. Integrit.* **17**, 924-933. https://doi.org/10.1016/j.prostr.2019.08.123.

Armaghani, D.J., Mohamad, E.T., Hajihassani, M., Yagiz, S. and Motaghedi, H. (2016a), "Application of several non-linear

prediction tools for estimating uniaxial compressive strength of granitic rocks and comparison of their performances", *Eng. Comput.*, **32**(2), 189-206. https://doi.org/10.1007/s00366-015-0410-5.

Armaghani, D.J., Mohamad, E.T., Momeni, E., Monjezi, M. and Narayanasamy, M.S. (2016b), "Prediction of the strength and elasticity modulus of granite through an expert artificial neural network", *Arab. J. Geosci.*, **9**(1), 48. https://doi.org/10.1007/s12517-015-2057-3.

Armaghani, D.J., Momeni, E. and Asteris, P.G. (2020), "Application of group method of data handling technique in assessing deformation of rock mass", *Metaheur. Comput. Appl.*, **1**(1), 1-18. http://doi.org/10.12989/mca.2020.1.1.001.

Asteris, P. G., Douvika, M. G., Karamani, C. A., Skentou, A. D., Chlichlia, K., Cavaleri, L., Daras, T., Armaghani, D.J. and Zaoutis, T.E. (2020), "A novel heuristic algorithm for the modeling and Risk Assessment of the COVID-19 pandemic phenomenon", *Comput. Model. Eng. Sci.*, **125**(2), 815-828. https://doi.org/10.32604/cmes.2020.013280.

Asteris, P.G. and Kolovos, K.G. (2017), "Self-compacting concrete strength prediction using surrogate models", *Neural Comput. Appl.*, 1-16. https://doi.org/10.1007/s00521-017-3007-7.

Asteris, P.G. and Mokos, V.G. (2019), "Concrete compressive Ssrength using artificial neural networks", *Neural Comput. Appl.*, 1-20. https://doi.org/10.1007/s00521-019-04663-2.

Asteris, P.G. and Plevris, V. (2013), "Neural network approximation of the masonry failure under biaxial compressive stress", *Proceedings of the 3rd South-East European Conference on Computational Mechanics (SEECCM III), an ECCOMAS and IACM Special Interest Conference*, Kos Island, Greece, June.

Asteris, P.G. and Plevris, V. (2016), "Anisotropic masonry failure criterion using artificial neural networks", *Neural Comput. Appl.*, 1-23. https://doi.org/10.1007/s00521-016-2181-3.

Asteris, P.G., Apostolopoulou, M., Armaghani, D.J., Cavaleri, L., Chountalas, A.T., Guney, D., Hajihassani, M., Hasanipanah, M., Khandelwal, M., Karamani, C., Koopialipoor, M., Kotsonis, E., Le, T.T., Lourenço, P.B., Ly, H.B., Moropoulou, A., Nguyen, H., Pham, B.T., Samui, P. and Zhou, J. (2020), "On the metaheuristic models for the prediction of cement-metakaolin mortars compressive strength", *Metaheur. Comput. Appl.*, **1**(1), 63-99. http://doi.org/10.12989/mca.2020.1.1.063.

Asteris, P.G., Roussis, P.C. and Douvika, M.G. (2017), "Feed-forward neural network prediction of the mechanical properties of sandcrete materials", *Sensors*, **17**(6), 1344. https://doi.org/10.3390/s17061344.

ASTM D2166 (2016), Standard Test Method for Unconfined Compressive Strength of Cohesive Soil, ASTM International, West Conshohocken, Pennsylvania, U.S.A.

Aydin, A. and Basu, A. (2005), "The Schmidt hammer in rock material characterization", *Eng. Geol.*, **81**(1), 1-14. https://doi.org/10.1016/j.enggeo.2005.06.006.

Barham, W.S., Rababah, S.R., Aldeeky, H.H. and Al Hattamleh, O.H. (2020), "Mechanical and physical based artificial neural network models for the prediction of the unconfined compressive strength of rock", *Geotech. Geol. Eng.*, **38**(5), 4779-4792. https://doi.org/10.1007/s10706-020-01327-0.

Bartlett, P.L. (1998), "The sample complexity of pattern classification with neural networks: The size of the weights is more important than the size of the network", *IEEE T. Inform. Theor.*, **44**(2), 525-536. https://doi.org/10.1109/18.661502.

Barton, N. (1973), "Review of a new shear-strength criterion for rock joints", *Eng. Geol.*, **7**(4), 287-332. https://doi.org/10.1016/0013-7952(73)90013-6.

Bozorgzadeh, N., Harrison, J.P. and Escobar, M.D. (2019), "Hierarchical Bayesian modelling of geotechnical data: Application to rock strength", *Géotechnique*, **69**(12), 1056-1070. https://doi.org/10.1680/jgeot.17.P.282.

Cavaleri, L., Asteris, P.G., Psyllaki, P.P., Douvika, M.G., Skentou, A.D. and Vaxevanidis, N.M. (2019), "Prediction of surface treatment effects on the tribological performance of tool steels using artificial neural networks", *Appl. Sci.*, **9**(14), 2788. https://doi.org/10.3390/app9142788.

Cavaleri, L., Chatzarakis, G.E., Di Trapani, F.D., Douvika, M.G., Roinos, K., Vaxevanidis, N.M. and Asteris, P.G. (2017), "Modeling of surface roughness in electro-discharge machining using artificial neural networks", *Adv. Mater. Res.*, **6**(2), 169-184. http://doi.org/10.12989/amr.2017.6.2.169.

Ceryan, N. and Samui, P. (2020), "Application of soft computing methods in predicting uniaxial compressive strength of the volcanic rocks with different weathering degree", *Arab. J. Geosci.*, **13**(7), 1-18. https://doi.org/10.1007/s12517-020-5273-4.

Ceryan, N., Okkan, U. and Kesimal, A. (2013), "Prediction of unconfined compressive strength of carbonate rocks using artificial neural networks", *Environ. Earth Sci.*, **68**(3), 807-819. https://doi.org/10.1007/s12665-012-1783-z.

Chaki, S., Takarli, M. and Agbodjan, W.P. (2008), "Influence of thermal damage on physical properties of a granite rock: Porosity, permeability and ultrasonic wave evolutions", *Construct. Build. Mater.*, **22**(7), 1456-1461. https://doi.org/10.1016/j.conbuildmat.2007.04.002.

Chen, H., Asteris, P.G., Armaghani, D.J., Gordan, B. and Pham, B.T. (2019), "Assessing dynamic conditions of the retaining wall using two hybrid intelligent models", *Appl. Sci.*, **9**, 1042. https://doi.org/10.3390/app9061042.

Ching, J., Li, K.H., Phoon, K.K. and Weng, M.C. (2018), "Generic transformation models for some intact rock properties", *Can. Geotech. J.*, **55**(12), 1702-1741. https://doi.org/10.1139/cgj-2017-0537

Çobanoğlu, İ. and Çelik, S.B. (2008), "Estimation of uniaxial compressive strength from point load strength, Schmidt hardness and P-wave velocity", *B. Eng. Geol. Environ.*, **67**(4), 491-498. https://doi.org/10.1007/s10064-008-0158-x.

Das, S.K., Samui, P. and Sabat, A.K. (2011), "Application of artificial intelligence to maximum dry density and unconfined compressive strength of cement stabilized soil", *Geotech. Geol. Eng.*, **29**(3), 329-342. https://doi.org/10.1007/s10706-010-9379-4.

Dehghan, S., Sattari, G.H., Chelgani, S.C. and Aliabadi, M.A. (2010), "Prediction of uniaxial compressive strength and modulus of elasticity for Travertine samples using regression and artificial neural networks", *Min. Sci. Technol.*, **20**(1), 41-46. https://doi.org/10.1016/S1674-5264(09)60158-7.

Diamantis, K., Bellas, S., Migiros, G. and Gartzos, E. (2011), "Correlating wave velocities with physical, mechanical properties and petrographic characteristics of peridotites from the central Greece", *Geotech. Geol. Eng.*, **29**(6), 1049. https://doi.org/10.1007/s10706-011-9436-7.

Diamantis, K., Gartzos, E. and Migiros, G. (2009), "Study on uniaxial compressive strength, point load strength index, dynamic and physical properties of serpentinites from Central Greece: Test results and empirical relations", *Eng. Geol.*, **108**(3-4), 199-207. https://doi.org/10.1016/j.enggeo.2009.07.002.

Ebdali, M., Khorasani, E. and Salehin, S. (2020), "A comparative study of various hybrid neural networks and regression analysis to predict unconfined compressive strength of travertine", *Innov. Infrastruct. Solutions*, **5**(3), 1-14. https://doi.org/10.1007/s41062-020-00346-3.

Ferentinou, M. and Fakir, M. (2017), "An ANN approach for the

prediction of uniaxial compressive strength, of some sedimentary and igneous rocks in eastern KwaZulu-Natal", *Procedia Eng*., **191**, 1117-1125. https://doi.org/10.1016/j.proeng.2017.05.286.

Franklin, J.A. and Dusseault, M.B (1991), *Rock Engineering Applications*, McGraw-Hill, New York, U.S.A.

Gavriilaki, E., Asteris, P.G., Touloumenidou, T., Koravou, E.E., Koutra, M., Papayanni, P.G., Karali, V., Papalexandri, A., Varelas, C., Chatzopoulou, F., Chatzidimitriou, M. and Anagnostopoulos, A. (2021), "Genetic justification of severe COVID-19 using a rigorous algorithm", *Clin. Immun*., **226**, 108726. https://doi.org/10.1016/j.clim.2021.108726

Goudie, A.S. (2006), "The Schmidt hammer in geomorphological research", *Progress Phys. Geography*, **30**(6), 703. https://doi.org/10.1177/0309133306071954.

Hawkins, A.B. (1998), "Aspects of rock strength", *B. Eng. Geol. Environ*., **57**(1), 17-30. https://doi.org/10.1007/s100640050017.

Heidari, M., Mohseni, H. and Jalali, S.H. (2018), "Prediction of uniaxial compressive strength of some sedimentary rocks by fuzzy and regression models", *Geotech. Geol. Eng*., **36**(1), 401-412. https://doi.org/10.1007/s10706-017-0334-5.

Hoek, E. and Brown, E.T. (1980), "Empirical strength criterion for rock masses", *J. Geotech. Geoenviron. Eng*., **106**, 15715. https://doi.org/10.1061/AJGEB6.0001029.

Hoek, E. and Brown, E.T. (1997), "Practical estimates of rock mass strength", *Int. J. Rock Mech. Min. Sci*., **34**(8), 1165-1186. https://doi.org/10.1016/S1365-1609(97)80069-X.

Hoek, E.(1983), "Strength of jointed rock masses", *Geotechnique*, **33**(3), 187-223. https://doi.org/10.1680/geot.1983.33.3.187.

Hoek, E., Carranza-Torres, C. and Corkum, B. (2002), "Hoek-Brown failure criterion-2002 edition", *Proc NARMS-Tac*., **1**(1), 267-273.

Hornik, K., Stinchcombe, M. and White, H. (1989), "Multilayer feedforward networks are universal approximators", *Neural Netw*., **2**, 359-366. https://doi.org/10.1016/0893-6080(89)90020-8.

index and physical tests", *J. Rock Mech. Geotech. Eng*., **12**(2), 256-268. https://doi.org/10.1016/j.jrmge.2019.08.001.

ISRM (2007). *The complete ISRM suggested methods for rock characterization, testing and monitoring: 1974-2006*, in *Suggested Methods Prepared by the Commission on Testing Method*s, International Society for Rock Mechanics, Turkish National Group; Ankara, Turkey.

Kahraman, S. (2001), "Evaluation of simple methods for assessing the uniaxial compressive strength of rock", *Int. J. Rock Mech. Min. Sci*., **38**(7), 981-994. https://doi.org/10.1016/S1365-1609(01)00039-9.

Karlik, B. and Olgac, A.V. (2011), "Performance analysis of various activation functions in generalized MLP architectures of neural networks", *Int. J. Artif. Intell. Expert Syst*., **1**(4), 111-122.

Kashani, A.R., Gandomi, M., Camp, C.V., Rostamian, M. and Gandomi, A.H. (2020), "Metaheuristics in civil engineering: A review", *Metaheur. Comput. Appl*., **1**(1), 19-42. http://doi.org/10.12989/mca.2020.1.1.019

Kechagias, J., Tsiolikas, A., Asteris, P. and Vaxevanidis, N. (2018), "Optimizing ANN performance using DOE: Application on turning of a titanium alloy", *Proceedings of the 22nd International Conference on Innovative Manufacturing Engineering and Energy*, Chisinau, Moldova, May.

Kelsall, P.C., Watters, R.J. and Franzone, G. (1986), "Engineering characterization of fissured, weathered dolerite and vesicular basalt", *Proceedings of the 27th U.S. Symposium on Rock Mechanics*, Tuscaloosa, Alabama, U.S.A., June.

Khandelwal, M. (2013), "Correlating P-wave velocity with the physico-mechanical properties of different rocks", *Pure Appl. Geophys*., **170**(4), 507-514. https://doi.org/10.1007/s00024-012-0556-7.

Khandelwal, M. and Singh, T.N. (2009), "Correlating static properties of coal measures rocks with P-wave velocity", *Int. J. Coal Geol*., **79**(1-2), 55-60. https://doi.org/10.1016/j.coal.2009.01.004.

Khandelwal, M., Armaghani, D.J., Faradonbeh, R.S., Ranjith, P.G. and Ghoraba, S. (2016), "A new model based on gene expression programming to estimate air flow in a single rock joint", *Environ. Earth. Sci*., **75**(9), 739-786. https://doi.org/10.1007/s12665-016-5524-6.

Kılıç, A. and Teymen, A. (2008), "Determination of mechanical properties of rocks using simple methods", *B. Eng. Geol. Environ*., **67**(2), 237. https://doi.org/10.1007/s10064-008-0128-3.

Li, D., Armaghani, D.J., Zhou, J., Lai, S.H. and Hasanipanah, M. (2020), "A GMDH predictive model to predict rock material strength using three non-destructive tests", *J. Nondestruct. Eval*., **39**(4), 1-14. https://doi.org/10.1007/s10921-020-00725-x.

Liang, M., Mohamad, E.T., Faradonbeh, R.S., Armaghani, D.J. and Ghoraba, S. (2016), "Rock strength assessment based on regression tree technique", *Eng. Comput*., **32**(2), 343-354. https://doi.org/10.1007/s00366-015-0429-7.

Madhubabu, N., Singh, P.K., Kainthola, A., Mahanta, B., Tripathy, A. and Singh, T.N. (2016), "Prediction of compressive strength and elastic modulus of carbonate rocks", *Measurement*, **88**, 202-213. https://doi.org/10.1016/j.measurement.2016.03.050.

Marinos, P. and Hoek, E. (2000), "GSI: A geologically friendly tool for rock mass strength estimation", *Proceedings of the ISRM International Symposium,* Melbourne, Australia, November.

Minaeian, B. and Ahangari, K. (2013), "Estimation of uniaxial compressive strength based on P-wave and Schmidt hammer rebound using statistical method", *Arab. J. Geosci*., **6**(6), 1925-1931. https://doi.org/10.1007/s12517-011-0460-y.

Mishra, D.A. and Basu, A. (2013), "Estimation of uniaxial compressive strength of rock materials by index tests using regression analysis and fuzzy inference system", *Eng. Geol*., **160**, 54-68. https://doi.org/10.1016/j.enggeo.2013.04.004.

Momeni, E., Armaghani, D.J., Hajihassani, M. and Amin, M.F.M. (2015), "Prediction of uniaxial compressive strength of rock samples using hybrid particle swarm optimization-based artificial neural networks", *Measurement*, **60**, 50-63. https://doi.org/10.1016/j.measurement.2014.09.075.

Moradian, Z.A. and Behnia, M. (2009), "Predicting the uniaxial compressive strength and static Young's modulus of intact sedimentary rocks using the ultrasonic test", *Int. J. Geomech*., **9**(1), 14-19. https://doi.org/10.1061/(ASCE)1532-3641(2009)9:1(14).

Moussas, V.M. and Diamantis, K. (2021), "Predicting uniaxial compressive strength of serpentinites through physical, dynamic and mechanical properties using neural networks", *J. Rock Mech. Geotech. Eng*., **13**(1), 167-175. https://doi.org/10.1016/j.jrmge.2020.10.001.

Ng, I.T., Yuen, K.V. and Lau, C.H. (2015), "Predictive model for uniaxial compressive strength for Grade III granitic rocks from Macao", *Eng. Geol*., **199**, 28-37. https://doi.org/10.1016/j.enggeo.2015.10.008.

Nikoo, M., Hadzima-Nyarko, M., KarloNyarko, E. and Nikoo, M. (2018), "Determining the natural frequency of cantilever beams using ANN and heuristic search", *Appl. Artif. Intell*., **32**(3), 309-334. https://doi.org/10.1080/08839514.2018.1448003.

Nikoo, M., Ramezani, F., Hadzima-Nyarko, M., Nyarko, E.K. and Nikoo, M. (2016), "Flood-routing modeling with neural network optimized by social-based algorithm", *Nat. Hazards*, **82**(1), 1-24. https://doi.org/10.1007/s11069-016-2176-5.

Nikoo, M., Sadowski, L., Khademi, F. and Nikoo, M. (2017), "Determination of damage in reinforced concrete frames with shear walls using self-organizing feature map", *Appl. Comput. Intell. Soft Comput.*, 1-10. https://doi.org/10.1155/2017/3508189.

Psyllaki, P., Stamatiou, K., Iliadis, I., Mourlas, A., Asteris, P. and Vaxevanidis, N. (2018), "Surface treatment of tool steels against galling failure", *Proceedings of the 5th International Conference of Engineering against failure,* Chios, Greece, June.

Rahimi, I., Gandomi, A.H., Asteris, P.G. and Chen, F. (2021), "Analysis and prediction of COVID-19 using SIR, SEIQR, and machine learning models: Australia, Italy, and UK Cases", *Information*, **12**(3), 109. https://doi.org/10.3390/info12030109.

Samui, P. (2008), "Support vector machine applied to settlement of shallow foundations on cohesionless soils", *Comput. Geotech.*, **35**(3), 419-427. https://doi.org/10.1016/j.compgeo.2007.06.014.

Samui, P. and Kothari, D.P. (2011), "Utilization of a least square support vector machine (LSSVM) for slope stability analysis", *Scientia Iranica,* **18**(1), 53-58. https://doi.org/10.1016/j.scient.2011.03.007.

Singh, T.N., Kainthola, A. and Venkatesh, A. (2012), "Correlation between point load index and uniaxial compressive strength for different rock types", *Rock Mech. Rock Eng.*, **45**(2), 259-264. https://doi.org/10.1007/s00603-011-0192-z.

Tandon, R.S. and Gupta, V. (2015), "Estimation of strength characteristics of different Himalayan rocks from Schmidt hammer rebound, point load index, and compressional wave velocity", *B. Eng. Geol. Environ.*, **74**(2), 521-533. https://doi.org/10.1007/s10064-014-0629-1.

Teymen, A. and Mengüç, E.C. (2020), "Comparative evaluation of different statistical tools for the prediction of uniaxial compressive strength of rocks", *Int. J. Min. Sci. Technol.*, **30**(6), 785-797. https://doi.org/10.1016/j.ijmst.2020.06.008.

Thuro, K., Plinninger, R.J., Zäh, S. and Schütz, S. (2001), "Scale effects in rock strength properties. Part 1: Unconfined compressive test and Brazilian test", *Proceedings of the ISRM Regional Symposium*, *EUROCK 2001*, Espoo, Finland, June.

Tsiambaos, G. and Sabatakakis, N. (2004), "Considerations on strength of intact sedimentary rocks", *Eng. Geol.*, **72**(3-4), 261-273. https://doi.org/10.1016/j.enggeo.2003.10.001.

Tsiambaos, G. and Sabatakakis, N. (2004), "Considerations on strength of intact sedimentary rocks", *Eng. Geol.*, **72**(3-4), 261-273. https://doi.org/10.1016/j.enggeo.2003.10.001.

Tuğrul, A. (2004), "The effect of weathering on pore geometry and compressive strength of selected rock types from Turkey", *Eng. Geol.*, **75**(3-4), 215-227. https://doi.org/10.1016/j.enggeo.2004.05.008.

Tuğrul, A. and Zarif, I.H. (1999), "Correlation of mineralogical and textural characteristics with engineering properties of selected granitic rocks from Turkey", *Eng. Geol.*, **51**(4), 303-317. https://doi.org/10.1016/S0013-7952(98)00071-4.

Vasconcelos, G., Lourenço, P.B., Alves, C.A. and Pamplona, J. (2007), "Prediction of the mechanical properties of granites by ultrasonic pulse velocity and Schmidt hammer hardness", *Proceedings of the North American Masonry Conference,* St. Louis, Missouri, October.

Vasconcelos, G., Lourenço, P.B., Alves, C.A.S. and Pamplona, J. (2008), "Ultrasonic evaluation of the physical and mechanical properties of granites", *Ultrasonics,* **48**(5), 453-466. https://doi.org/10.1016/j.ultras.2008.03.008.

Wang, M., Wan, W. and Zhao, Y. (2020), "Prediction of the uniaxial compressive strength of rocks from simple index tests using a random forest predictive model", *Comptes Rendus Mécanique*, **348**(1), 3-32. https://doi.org/10.5802/crmeca.3.

Wu, H.H. and Wu, S. (2009), "Various proofs of the Cauchy-Schwarz Inequality", *Octogon Math. Magazine*, **17**(1), 221-229.

Xu, H., Zhou, J., Asteris, P.G., Armaghani, D.J. and Tahir, M. (2019), "Supervised machine learning techniques to the prediction of tunnel boring machine penetration rate", *Appl. Sci.*, **9**(18), 3715. https://doi.org/10.3390/app9183715.

Yagiz, S., Sezer, E.A. and Gokceoglu, C. (2012), "Artificial neural networks and nonlinear regression techniques to assess the influence of slake durability cycles on the prediction of uniaxial compressive strength and modulus of elasticity for carbonate rocks", *Int. J. Numer. Anal. Met.*, **36**(14), 1636-1650. https://doi.org/10.1002/nag.1066.

Yaşar, E. and Erdogan, Y. (2004a), "Correlating sound velocity with the density, compressive strength and Young's modulus of carbonate rocks", *Int. J. Rock Mech. Min. Sci.*, **41**(5), 871-875. https://doi.org/10.1016/j.ijrmms.2004.01.012.

Yaşar, E. and Erdoğan, Y. (2004b), "Estimation of rock physicomechanical properties using hardness methods", *Eng. Geol.*, **71**(3-4), 281-288. https://doi.org/10.1016/S0013-7952(03)00141-8.

Yesiloglu-Gultekin, N., Gokceoglu, C. and Sezer, E.A. (2013), "Prediction of uniaxial compressive strength of granitic rocks by various nonlinear tools and comparison of their performances", *Int. J. Rock Mech. Min. Sci.*, **62**, 113-122. https://doi.org/10.1016/j.ijrmms.2013.05.005.

Yılmaz, I. and Yuksek, A.G. (2008), "An example of artificial neural network (ANN) application for indirect estimation of rock parameters", *Rock Mech. Rock Eng.*, **41**(5), 781-795. https://doi.org/10.1007/s00603-007-0138-7.

Yilmaz, I. and Yuksek, G. (2009), "Prediction of the strength and elasticity modulus of gypsum using multiple regression, ANN, and ANFIS models", *Int. J. Rock Mech. Min. Sci.*, **46**(4), 803-810. https://doi.org/10.1016/j.ijrmms.2008.09.002.

Yurdakul, M. and Akdas, H. (2013), "Modeling uniaxial compressive strength of building stones using non-destructive test results as neural networks input parameters", *Constr. Build. Mater.*, **47**, 1010-1019. https://doi.org/10.1016/j.conbuildmat.2013.05.109.

Zeng, J., Asteris, P.G., Mamou, A.P., Mohammed, A.S., Golias, E.A., Armaghani, D.J., Faizi, K. and Hasanipanah, M. (2021), "The effectiveness of ensemble-neural network techniques to predict peak uplift resistance of buried pipes in reinforced Sand", *Appl. Sci.*, **2**(11), 908. https://doi.org/10.3390/app11030908.

Zhang, H., Nguyen, H., Bui, X.N., Pradhan, B., Asteris, P.G., Costache, R. and Aryal, J.A. (2021), "A generalized artificial intelligence model for estimating the friction angle of clays in evaluating slope stability using a deep neural network and Harris Hawks optimization algorithm", *Eng. Comput.*, 1-14. https://doi.org/10.1007/s00366-020-01272-9.

Zhao, J., Nguyen, H., Nguyen-Thoi, T., Asteris, P.G. and Zhou, J. (2021), "Improved Levenberg–Marquardt backpropagation neural network by particle swarm and whale optimization algorithms to predict the deflection of RC beams", *Eng. Comput.*, 1-23. https://doi.org/10.1007/s00366-020-01267-6.

CC

Notation

ANN(s)	Artificial Neural Network(s)
BHM	Bayesian Hierarchical Modelling
BPNN	Back Propagation Neural Network

Co	Competitive transfer function
GP	Genetic Programming
CS	Compressive Strength
HTS	Hyperbolic Tangent Sigmoid transfer function
Li	Linear transfer function
LS	Log-Sigmoid transfer function
MAPE	Mean Absolute Percentage Error
MSE	Mean Square Error
NN(s)	Neural Network(s)
NRB	Normalized Radial Basis transfer function
n_e	Effective porosity
PLi	Positive Linear transfer function
R	Pearson correlation coefficient
RB	Radial Basis transfer function
SM	Soft Max transfer function
SSE	Sum Square Error
SP	Superplasticizer
SSL	Symmetric Saturating Linear transfer function
TB	Triangular Basis transfer function
UCS	Unconfined Compressive Strength
V_p	Pulse velocity